

# **A Dual Spectrum Core for the ATW – Preliminary Feasibility Study**

Nathan Stone, Ehud Greenspan, Paul Chambre' and Micah Lowenthal  
Department of Nuclear Engineering  
University of California  
Berkeley, CA 94720  
nstone@nuc.berkeley.edu;gehud@nuc.berkeley.edu

## **ABSTRACT**

One of the primary goals of the Accelerator Transmutation of Waste (ATW) reactor being proposed by the Los Alamos National Laboratory is to reduce the radiological hazard of the high-level waste destined for disposal in the Yucca Mountain Repository (YMR). The purpose of the present study is to search for improved ATW core designs that will reduce the long term inventory of  $^{237}\text{Np}$  – a dominant contributor to the YMR long-term radiological hazard. Core composition changes in the ATW reactor are modeled using MCNP and a simple burnup model. In order to maximize the destruction of  $^{237}\text{Np}$  and its precursors ( $^{241}\text{Pu}$  and  $^{241}\text{Am}$ ), Np and Am are partitioned from the rest of the actinides and loaded into an outer zone of the core where  $\text{ZrH}_{1.6}$  is added as a moderator. The remaining actinides are loaded into an inner, unmoderated zone of the core. Both zones are Pb cooled. It is found that this ATW two-zone (ATW-TZ) core can significantly increase the fractional transmutation of  $^{237}\text{Np}$  and its precursors. This increase is by a factor of 4 for a single-batch fuel cycle and by a factor of 2.4 for a 3-batch fuel cycle. For the same fractional transmutation, the dual-spectrum core can reduce the burnup reactivity swing by more than a factor of 2.

## **1. INTRODUCTION**

The Accelerator-driven Transmutation of Waste (ATW) reactor<sup>1</sup> uses a sub-critical reactor core that is driven by a spallation neutron source. It is to transmute spent fuel from light water reactors (LWR) and military reactors. Possible benefits of the system include reduction of quantity of actinides in the high-level-waste and power generation. Implications of the former include reduction of long-term radiological hazards within a repository system, and increasing the proliferation resistance of a repository.

In the ATW system proposed by Los Alamos National Labs (LANL),<sup>1</sup> the actinides extracted from the spent fuel would be fabricated into zirconium-based fuel elements. Molten lead is proposed as the primary coolant and as the target for the spallation neutron source. The spallation source is located at the center of the reactor core. The core is always sub-critical ( $k_{\text{eff}} \leq 0.98$ )

during operation and power is maintained by increasing the proton beam current as  $k_{\text{eff}}$  decreases with burnup.

The proposed fuel cycle<sup>1</sup> uses a fuel shuffling scheme where fresh fuel is loaded into the core region furthest from the spallation source and then is moved to a closer region and then to the innermost region as its reactivity decreases. New fuel is added every 110-days and is extracted after 330 days of irradiation. The extracted fuel is recycled after fission product removal. Ideally, this process would be repeated until the entire actinide content of the waste had been transmuted and only fission products would enter the repository. In reality, in each reprocessing cycle a fraction of the actinides cannot be recovered and ends up in the waste stream. These eventually must be disposed of in a repository. Although constituting a small fraction of the initial inventory, these residual actinides can still become the dominant source of radiological hazard in a repository system.

Using the Yucca Mountain Repository (YMR) as a reference disposal system, we found in previous work<sup>2,3</sup> that  $^{237}\text{Np}$  is likely to be the dominant contributor to the long-term radiological hazard among the actinides from the ATW reference design waste stream. Since one of the stated aims of the ATW technology proposed by LANL is to reduce the radiological hazard of the high-level waste destined for disposal in the proposed YMR, this study seeks to minimize the final inventory of  $^{237}\text{Np}$  that is deposited into the YMR. Because  $^{237}\text{Np}$  can be formed through the decay of  $^{245}\text{Cm}$ ,  $^{241}\text{Pu}$ ,  $^{241}\text{Am}$ , and  $^{237}\text{U}$ , we consider the evolution of the inventory of these isotopes. The initial inventories of  $^{245}\text{Cm}$  and  $^{237}\text{U}$  are negligible compared to the other precursors of  $^{237}\text{Np}$ . Thus, the quantity used to characterize the long-term  $^{237}\text{Np}$  inventory is the sum of  $^{241}\text{Pu}$ ,  $^{241}\text{Am}$ , and  $^{237}\text{Np}$  inventories in the ATW waste stream.

For the reference ATW reactor design, a hard neutron spectrum was chosen because most actinides have a high fission-to-capture ratio at higher neutron energies. On the other hand,  $^{241}\text{Am}$  and  $^{237}\text{Np}$  can also be transmuted by capture reactions, as these reactions do not produce other problematic actinides. It turns out that  $^{241}\text{Am}$  and  $^{237}\text{Np}$  both have a very large epithermal and thermal capture cross sections; they are orders of magnitude larger than fission or capture cross sections at the hard spectrum of the reference ATW design.

This study explores the possibility of increasing the transmutation efficiency of  $^{237}\text{Np}$  and  $^{241}\text{Am}$  by irradiating Np and Am in a soft spectrum zone of the core. Specifically, we are considering a dual-spectrum core in which the Np and Am are partitioned from the rest of the actinides and loaded into a soft spectrum zone. The rest of the actinides are loaded into a hard spectrum zone, as in the reference ATW<sup>1</sup>. Had we irradiated Pu in a soft spectrum, large inventories of  $^{241}\text{Pu}$  would have been produced due to the large capture cross sections of  $^{240}\text{Pu}$  and  $^{239}\text{Pu}$ .

As this is a preliminary feasibility study, a simple but illuminating model is used for the burnup analysis. This model is described in Sec. 2. Section 3 describes the geometry and composition of the cores studied. The results obtained are presented in Sec. 4 and further discussed in Sec. 5.

## 2. COMPUTATIONAL MODEL

A simplified transmutation and decay chain, shown in Fig. 1, was used for calculating the evolution of the inventories of  $^{237}\text{Np}$  and its important precursors. The calculations were done by solving a set of 16 coupled rate equations. A typical rate equation is presented in Eq. 1; it is for  $^{237}\text{Np}$ . The symbol for an isotope (e.g.,  $^{241}\text{Am}$ ) represents the number of moles of that isotope.

$$\frac{dNp^{237}(t)}{dt} = -D_{(\lambda+a)}^{Np237} Np^{237}(t) + P_{(n,2n)}^{Np237} U^{238}(t) + P_{(n,\gamma)}^{Np237} U^{236}(t) + P_{(\lambda)}^{Np237} Am^{241}(t) \quad (1)$$

The “D” and “P” parameters in Eq. (1) are, respectively, the “destruction coefficients” and “production coefficients”. The destruction coefficient in Eq. (1) is

$$D^{Np237} = \lambda^{Np237} + \sigma_a^{Np237} \Phi \quad (2)$$

where  $\lambda$  is the radioactive decay constant of  $^{237}\text{Np}$ ,  $\sigma_a$  is its effective one group microscopic absorption cross section and  $\Phi$  is the total flux the  $^{237}\text{Np}$  is exposed to. The production coefficients in Eq. (1) are

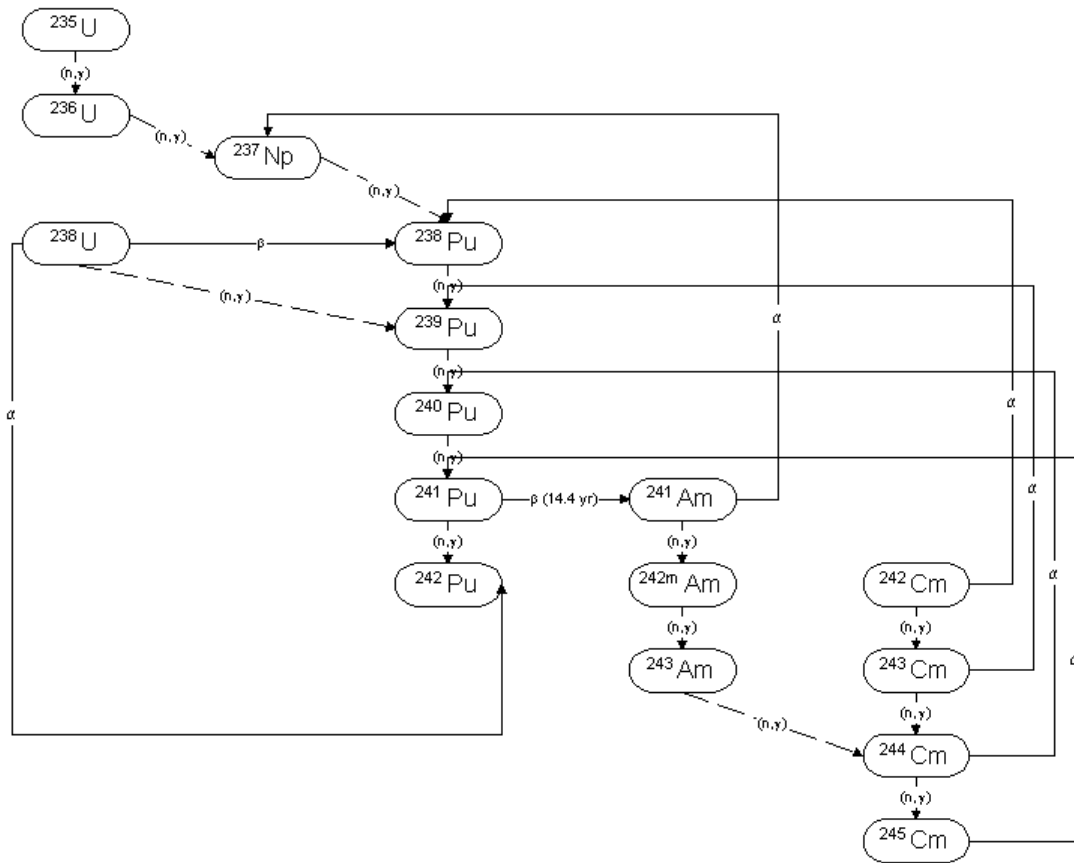


Figure 1. The 16-member destruction and production chain used for burnup analysis.

$$P_{(n,2n)}^{Np237} = \sigma_{n,2n}^{U238} \Phi , \quad P_{(n,\gamma)}^{Np237} = \sigma_{n,\gamma}^{U236} \Phi , \quad \text{and} \quad P_{(\lambda)}^{Np237} = \lambda^{Am241} . \quad (3)$$

The effective one group cross sections needed for the destruction and production coefficients are obtained by averaging the energy dependent cross sections with the average spectrum in the zone considered.

$$\sigma \equiv \frac{\sigma(E) \cdot \Phi(E) \cdot dE}{\Phi(E) \cdot dE} \quad (4)$$

The tallies representing the numerator and denominator of Eq. (4) are generated using MCNP.

The flux amplitude needed for calculating the production and destruction coefficients of the type shown in Eqs. (2) and (3) is obtained by assuming that the core maintains constant power for the duration of the fuel cycle. The total core power of the ATW reference core is 2.22 GW<sub>th</sub>. This condition implies that the average flux amplitude in Zone 1 is

$$\Phi_1 = \frac{2.22 \times 10^9 (W) \cdot 6.242 \times 10^{12} (MeV / W / s)}{200 (MeV / f) \cdot N_A \cdot \{\Sigma_1 + R \cdot \Sigma_2\}} \quad (5)$$

where  $N_A$  is Avogadro's number,  $\Sigma_x$  is the sum over all actinides of  $[N_{Mx}(i) \sigma_{fx}(i)]$ .  $N_{Mx}(i)$  is the total number of moles of actinide  $i$  in Zone  $x$  ( $x = 1$  or  $2$ ); it is generated by MCNP. The average flux amplitude in Zone 2 is taken to be  $\Phi_2 = R \Phi_1$  where  $R$  is the ratio of the flux in Zone 2 to the flux in Zone 1.  $R$  is calculated by MCNP.

Burnup calculations were made by solving the coupled set of 16 rate equations for a relatively small burnup step. After each burnup step a new set of destruction coefficients, production coefficients and flux amplitudes are calculated and the set of rate equations are resolved.

The solution of the rate equations was done with MS EXCEL. Consider, first, an isotope having no production term the inventory of which at the beginning of the time step is  $N(0)$ . The amount of this isotope transmuted in time step  $\Delta t$  is calculated from the exact analytic

$$\Delta N(\Delta t) = N(0) \cdot (1 - e^{(-D \cdot \Delta t)}) . \quad (6)$$

Consider, next, an isotope  $i$  that is produced by radiative capture in isotope  $i-1$ . The net change in the inventory of this isotope in the small time step  $\Delta t$  is calculated as from the approximate expression

$$\Delta N^i(\Delta t) = N^i(0) \cdot (1 - e^{(-D_{(a+\lambda)}^i \cdot \Delta t)}) + N^{i-1}(0) \cdot (1 - e^{(-P_{(n,\gamma)}^{i-1} \cdot \Delta t)}) . \quad (7)$$

Using 0.0005 year for the time steps, the numerical error introduced by the approximation is found to be less than 0.1%.

Table I summarizes the densities used for the core materials. The lead is assumed to be liquid at 800 K. The actinide density at the beginning of cycle (BOC) is calculated using the weight fractions defined in the next section. The actinide densities are recalculated at the beginning of each time step, accounting for the transmutation effects.

Table I. Core Materials and their Densities.

Material	Density (g/cm <sup>3</sup> )
Lead	10.39
304 SS Steel	7.98
ZrH <sub>1.6</sub>	5.611
Zr	6.511
Zone 1 Actinides	19.62
Zone 2 Actinides	15.94

The primary source of cross sections used for MCNP are the Evaluated Nuclear Data Files ENDF/B-VI and, when not available, ENDF/B-V. Most cross sections used are at room temperature (300 K) as high temperature cross sections were not provided in the library available to us. For ZrH<sub>1.6</sub> we used MCNP's S( $\alpha,\beta$ ) treatment assuming that the ZrH<sub>1.6</sub> is at 800 K. Table II shows the specific cross section library ID used for this study. The ID format is AAZZZ where AA is the atomic number and ZZZ is the atomic weight. 50c and 60c denote the origin of the cross section: ENDF/B-V or ENDF/B-VI. ZZZ of 000 represents the naturally occurring elements.

Table II. MCNP Cross Sections Used.

Isotope	Library ID	Isotope	Library ID
<sup>235</sup> U	92235.60c	<sup>244</sup> Cm	96244.60c
<sup>236</sup> U	92236.60c	<sup>245</sup> Cm	96245.60c
<sup>238</sup> U	92238.60c	<sup>246</sup> Cm	96246.60c
<sup>238</sup> Pu	94238.60c	<sup>230</sup> Th	90230.60c
<sup>239</sup> Pu	94239.60c	<sup>237</sup> Np	93237.60c
<sup>240</sup> Pu	94240.60c	Zr	40000.60c
<sup>241</sup> Pu	94241.60c	Fe	26000.50c
<sup>242</sup> Pu	94242.60c	Cr	24000.50c
<sup>241</sup> Am	95241.60c	Ni	28000.50c
<sup>242m</sup> Am	95242.50c	Mo	42000.50c
<sup>243</sup> Am	95243.60c	Pb	82000.50c
<sup>243</sup> Cm	96243.60c	<sup>1</sup> H	1001.60c

### 3. CORES STUDIED

We first modeled the ATW reference design as a basis for comparison and then modified it to create the dual spectra core model. We shall refer to the latter also as the ATW two-zone (ATW-TZ) core.

The ATW reference design is modeled as a three uniform homogeneous concentric radial zones. The spallation target region at the center of the core is modeled as a 30 cm diameter cylinder of liquid lead. The core is a 76-cm thick concentric cylinder containing a homogenized mixture of 22% SS-304, 33% lead coolant, and 45% fuel. The outermost zone is a 100-cm thick lead reflector. The fuel consists of 86% zirconium and 14% actinides. The initial actinide composition is given in the right column of Table III; it is that of LWR spent fuel that has undergone 30 years of cooling and from which 99.8% of the uranium has been removed. The core is 2 m in height and is reflected on both sides by a 1.5 m thick lead layer that extends from the system centerline to a radius of 191 cm.

The ATW-TZ core model is similar except that an additional zone (Zone 2), 24 cm in thickness, is introduced between the 76 cm thick core region (Zone 1) and the radial reflector. Zone 2 contains ZrH<sub>1.6</sub> rods that occupy a fraction of the 45 % available for the fuel. The fuel is made of Np and Am in Zr matrix. The fuel composition in Zone 1 of the dual spectra core is given in Table III.

Table III. BOL Fuel Composition.

Isotope	Weight fraction	
	ATW-TZ Zone 1	Reference
U235	2.43E-03	2.43E-03
U236	1.11E-03	1.11E-03
U238	2.16E-01	2.16E-01
Pu238	1.09E-02	1.09E-02
Pu239	4.11E-01	4.11E-01
Pu240	1.72E-01	1.72E-01
Pu241	3.03E-02	3.03E-02
Pu242	3.50E-02	3.50E-02
Am241	2.19E-04	7.30E-02
Am242 <sup>m</sup>	2.28E-07	7.62E-05
Am243	1.98E-05	6.60E-03
Cm243	1.94E-05	1.94E-05
Cm244	7.22E-04	7.22E-04
Cm245	7.34E-05	7.34E-05
Cm246	8.05E-06	8.05E-06
Th230	1.39E-06	1.39E-06
Np237	1.24E-04	4.12E-02
	Zone 2	
Am241	7.28E-02	----
Am242 <sup>m</sup>	7.59E-05	----
Am243	6.58E-03	----
Np237	4.11E-02	----
Total	1.00E+00	1.00E+00

## 4. RESULTS

### 4.1 ZONE 2 SPECTRUM OPTIMIZATION

A study was conducted to determine what is the best spectrum in the outer zone and how to achieve it. This study considered different hydride volume fractions in the second zone and tested the usefulness of adding a moderating buffer layer between the inner and outer fueled core zones. The buffer layer contained only  $\text{ZrH}_{1.6}$  (45%), coolant (33%), and steel (22%). The criterion used to measure how good is the spectrum is the value of the destruction coefficients of  $^{241}\text{Am}$  and  $^{237}\text{Np}$ . Figure 2 shows the  $^{241}\text{Am}$  and  $^{237}\text{Np}$  destruction coefficients for various cases as well as the flux ratio between Zone 2 (Soft) and Zone 1 (hard). For each case, the moderating layer thickness is given along with the volume fraction of  $\text{ZrH}_{1.6}$  in Zone 2.

It was found that the destruction coefficient of both  $^{241}\text{Am}$  and  $^{237}\text{Np}$  increases as the volume fraction of  $\text{ZrH}_{1.6}$  goes up. The  $^{237}\text{Np}$  destruction coefficient reaches a plateau when the  $\text{ZrH}_{1.6}$  volume fraction gets to approximately 40%. For  $^{241}\text{Am}$ , the plateau is reached beyond 60%  $\text{ZrH}_{1.6}$  (compare the values in Fig. 2 of the no buffer zone cases). Introduction of a buffer zone between Zone 1 and Zone 2 can increase the destruction coefficient of  $^{241}\text{Am}$ , provided it is thin – on the order of 1cm. A thin buffer zone can somewhat increase the destruction coefficient of  $^{237}\text{Np}$  provided the  $\text{ZrH}_{1.6}$  volume fraction in Zone 2 is less than 40%. On the other hand, the buffer zone increases the  $^{241}\text{Pu}$  production rate in Zone 1 (not shown in Fig. 2). For instance, with a 1cm thick buffer zone and 60%  $\text{ZrH}_{1.6}$  in Zone 2 (the 1cm/60% case), the  $^{241}\text{Am}$  destruction coefficient is 4.8% larger than in the 0cm/60% case. However, the increase in the number of slower neutrons reflected back into the hard-spectrum zone caused a 14.39% increase in the  $^{241}\text{Pu}$  production coefficient. Guided by these findings we decided to abandon the buffer layer. The optimal zirconium hydride rod fraction was found to be 70% of the volume available for fuel (45% of Zone 2 volume); it has been used for the analysis that follows.

Figure 3 shows the neutron spectrum averaged over the volume of Zone 1 and Zone 2 of a core having 70%  $\text{ZrH}_{1.6}$  in Zone 2. Also shown in Fig. 3 is the average neutron spectrum in the reference, single zone core. It is observed that the spectrum in Zone 1 of the TZ core is basically identical to the spectrum of the reference design core. The optimal spectrum in Zone 2 has a significant component of epithermal neutrons and only a small fraction of thermal neutrons.

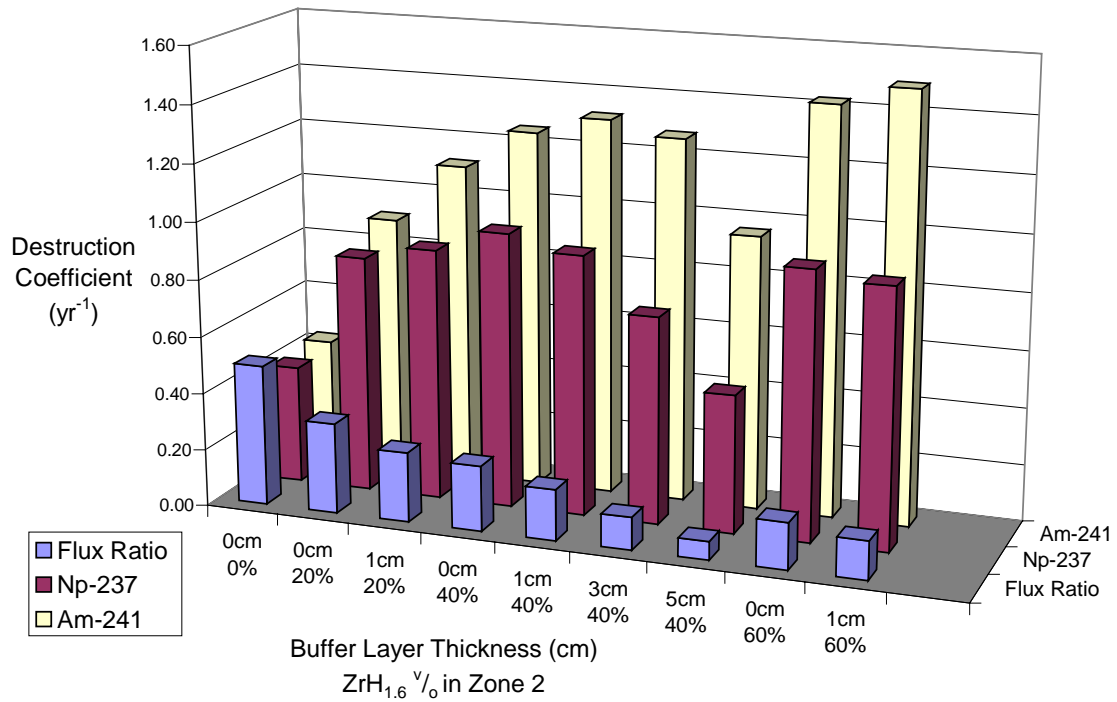


Figure 2. Destruction coefficients of <sup>237</sup>Np and <sup>241</sup>Am in Zone 2 of the reference TZ core along with Zone 2 to Zone 1 average flux ratio.

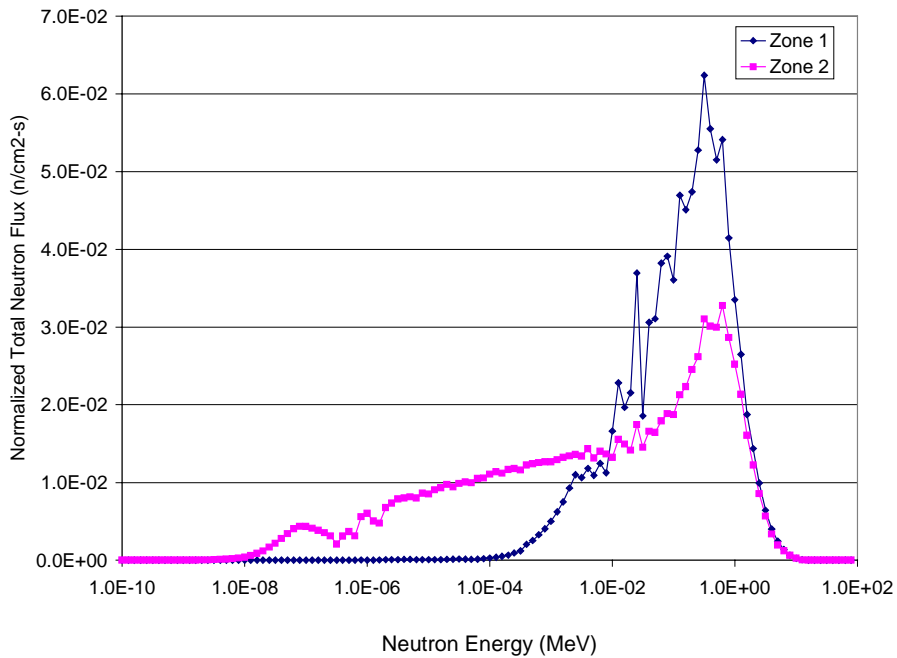


Figure 3. ATW-TZ normalized neutron spectrum for Zone 1 and Zone 2 compared with the spectrum for the ATW reference design. Zone 2 has 70 % ZrH<sub>1.6</sub>.

## 4.2 TZ CORE PERFORMANCE ANALYSIS

The performance of the ATW-TZ core is compared to that of the ATW reference core using the burnup model described in Sec. 2 and considering two characteristics: the fractional transmutation and  $k_{\text{eff}}$  variation with burnup. The fractional transmutation of a given isotope is defined as one minus the ratio of the inventory of this isotope found in the fuel discharged from the core to the inventory of this isotope initially loaded into the core. The ATW reference core cycle duration of 110-days or 0.30 years is limited by  $k_{\text{eff}}$  drop from 0.98 to 0.92. This analysis assumes that there is no fuel shuffling in the core; the fuel in each zone is exposed to the average zone flux.

Figure 4 compares the change in  $k_{\text{eff}}$  as a function of time in the ATW-TZ core and the ATW reference core. It is found that the ATW-TZ core can run for 0.45 years for a  $\Delta k_{\text{eff}}$  of -0.06. As a result, for the same burnup reactivity swing the TZ core enables obtaining close to 50% higher burnup of the discharged fuel. This can significantly reduce the amount of actinides that will get into the waste stream.

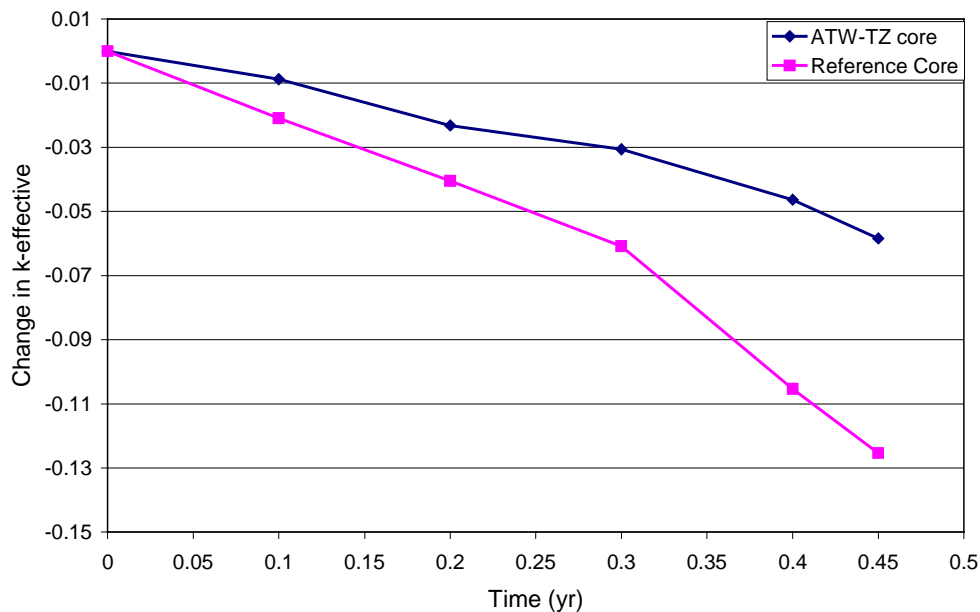


Figure 4. Change in  $k_{\text{eff}}$  with ATW operation time for the TZ and reference cores.

The dominant reason for the flatter burnup reactivity swing of the TZ core is the buildup of  $^{242\text{m}}\text{Am}$  in the outer, soft spectrum zone. Radiative capture in  $^{241}\text{Am}$  results in production of either  $^{242\text{m}}\text{Am}$  (88%) or  $^{242}\text{Cm}$  (12%).  $^{242\text{m}}\text{Am}$  has a large average fission cross section in the spectrum of Zone 2. Since the  $^{242\text{m}}\text{Am}$  inventory builds up with burnup, it partially compensates for the reactivity loss associated with the depletion of  $^{239}\text{Pu}$  and other actinides thus flattening the burnup reactivity swing.

At the beginning of the cycle, Zone 2 contributes only a small fraction of the total core power. As  $^{242\text{m}}\text{Am}$  builds up, the contribution of Zone 2 increases. Figure 5 shows the power-generation

evolution in the two core zones; the total core power is constant at 2.22 GW<sub>th</sub>. It is found that the contribution of Zone 2 builds up to 41% of the total core power. With such a large increase in power, Zone 2 power density becomes a concern. In order to keep Zone 2 power density within the constraint of 350 w/cm<sup>3</sup>, we increased the number of fuel rods, moderator rods and volume of Zone 2 by a factor of 2. The weight % of fuel in the Zr matrix was reduced by a factor of 2 to conserve the total fuel inventory in Zone 2.

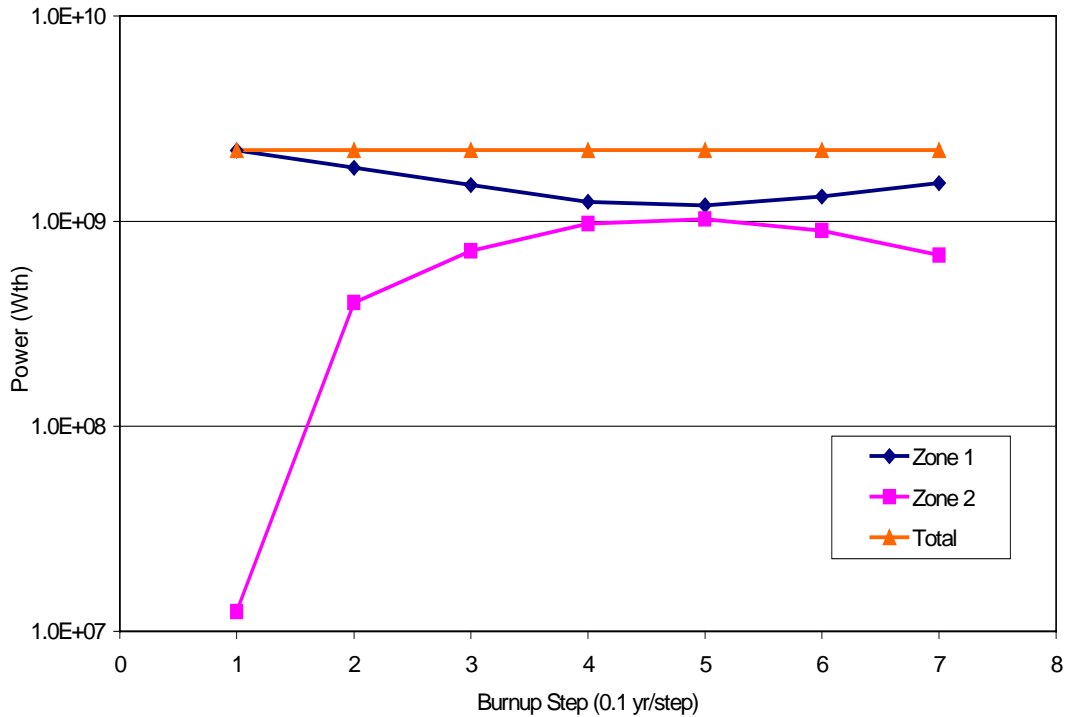


Figure 5. Evolution of the power generation in the ATW-TZ core.

Table IV shows the power density at the beginning of each burnup time step in both zones of the modified TZ core. It is observed that the maximum power density in Zone 2 does not exceed the BOC power density of Zone 1. But there is a significant swing in the power density from the inner to the outer zone.

Since the destruction and production coefficients are directly proportional to the flux, the buildup of <sup>242m</sup>Am and <sup>238</sup>Pu dramatically increases the destruction coefficients in Zone 2. The evolution of the destruction coefficients for <sup>237</sup>Np and <sup>241</sup>Am are shown in Figure 6.  $k_{eff}$  drops below 0.92 during the fifth burnup step. Steps 6 and 7 are shown only for illustrating the trends.

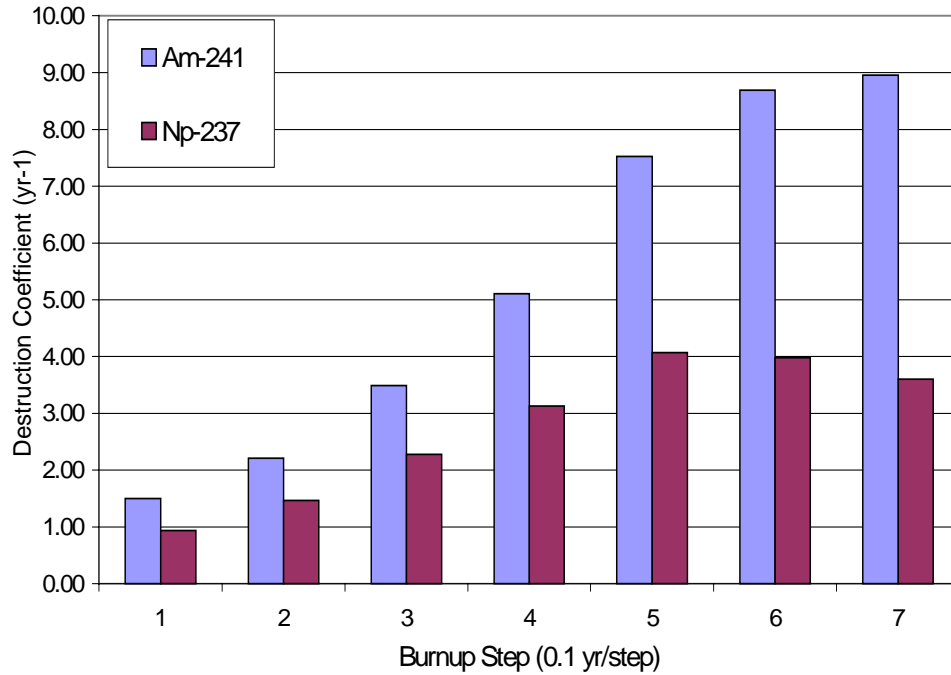


Figure 6. Zone 2 destruction coefficient dependence on burnup.

Figures 7 and 8 show the fractional inventory of  $^{237}\text{Np}$ ,  $^{241}\text{Am}$ , and  $^{241}\text{Pu}$  as function of ATW operating time in, respectively, the reference and the TZ (modified) cores. The curves end when the core change in  $k_{\text{eff}}$  equals  $-0.06$ . This happens after 0.3 year in the reference core and after 0.45 year in the TZ core. In 0.3 year the reference design transmutes 8.5% of the  $^{237}\text{Np}$  and 18.0% of the  $^{241}\text{Am}$  while producing 0.8% more  $^{241}\text{Pu}$  for a net reduction in  $^{237}\text{Np}$  and precursor mass inventory of 11.3%. For the same timeframe the ATW-TZ core transmutes 25.3% of the  $^{237}\text{Np}$  inventory and 44.0% of the  $^{241}\text{Am}$  inventory while producing 3.7% more  $^{241}\text{Pu}$  for a net reduction in  $^{237}\text{Np}$  and precursor mass inventory of 28.7%. This 2.5 folds increase in the fractional transmutation is solely due to the difference in the destruction coefficients. If the TZ core irradiation cycle was to be increased to 0.45 year, it would transmute 42.7% of the  $^{237}\text{Np}$  inventory and 68.1% of the  $^{241}\text{Am}$  inventory while producing an additional 6.3% of  $^{241}\text{Pu}$  giving a net reduction of  $^{237}\text{Np}$  precursor mass of 45.2% during a single cycle. This corresponds to a 4 folds increase in the transmutation efficiency.

At the end of each irradiation cycle, 1/3 of the fuel is discharged from the innermost region and newly fabricated fuel is loaded into the outermost region of the core. This makes the total fuel irradiation time between reprocessing of 330 days.

Assuming that the irradiation cycle extends over 3 fuel shufflings as in the reference LANL design<sup>1</sup>, and assuming space-independent flux within Zone 1 and Zone 2, we find the following: (a) The reference design will transmute 23.3% of the  $^{237}\text{Np}$  inventory and 44.8% of the  $^{241}\text{Am}$  inventory while producing 2.6% more  $^{241}\text{Pu}$ , for a net  $^{237}\text{Np}$  and precursor mass reduction of 28.4%. (b) The ATW-TZ core would transmute 58.3% of the  $^{237}\text{Np}$  inventory and 82.4% of the  $^{241}\text{Am}$  inventory while producing 11.8% more  $^{241}\text{Pu}$ , for a net  $^{237}\text{Np}$  and precursor mass

reduction of 57.2%. Both above cases correspond to a total irradiation time of 0.9 years. (c) When the irradiation cycle is  $(0.45 \times 3 =) 1.35$  years, the ATW-TZ core will transmute 81.2% of the  $^{237}\text{Np}$  inventory and 96.7% of the  $^{241}\text{Am}$  inventory while producing 20.2% more  $^{241}\text{Pu}$  for a net transmutation of 69.4% of the  $^{237}\text{Np}$  and precursor mass. This is a factor of 2.4 increase in the transmutation efficiency relative to the reference design.

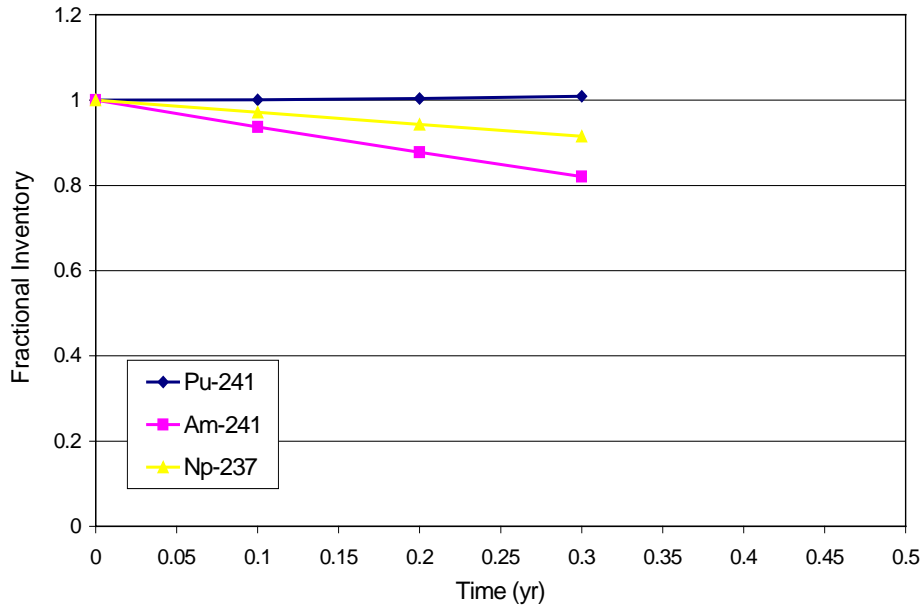


Figure 7. Transmutation performance of the ATW reference core.

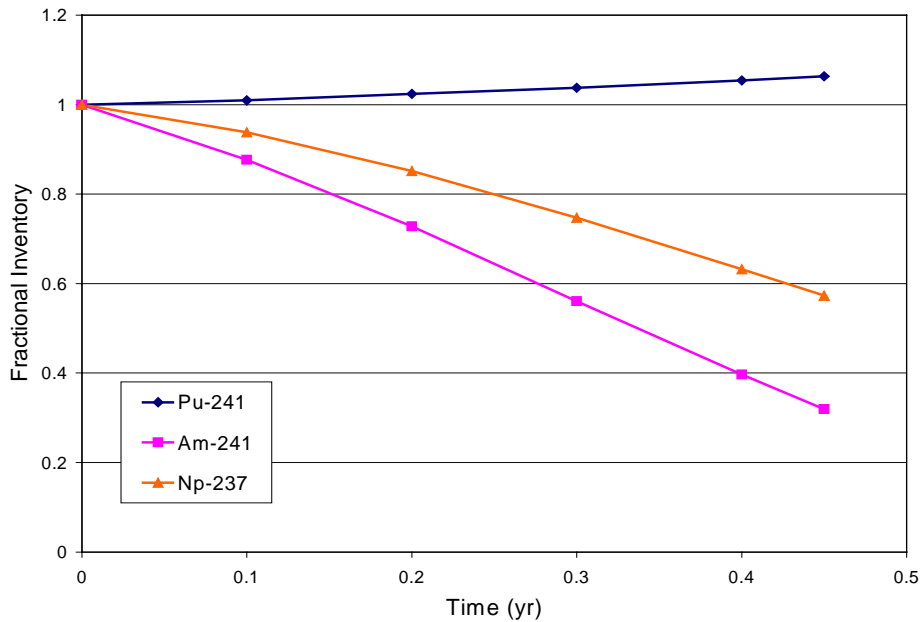


Figure 8. Transmutation performance of the ATW-TZ core.

Rather than maximizing the transmutation efficiency for a  $\Delta k_{\text{eff}} = -0.06$ , it is possible to benefit from the dual spectrum core for flattening of the burnup reactivity swing. Consider, for example, the single batch fuel cycle. Its duration in the reference core is 0.3 year. If the dual spectrum core was to operate for 0.3 year cycles,  $\Delta k_{\text{eff}}$  will be only  $-0.03$  (See Fig. 4) – half that of the reference core. This smaller burnup reactivity swing might have a significant economic benefit. As shown earlier in this section, this benefit can come along with an increase in the transmutation efficiency. If the ATW-TZ was to operate so as to give the same fractional transmutation as obtained with the reference ATW, the burnup reactivity swing would be reduced by more than a factor of 2.

## 5. DISCUSSION

Among the assumptions incorporated in our simple model, we identified two that deserve a careful investigation. The first assumption is the neglect of the effect of fission-product buildup in, primarily, Zone 2 on the core reactivity. At the time that Zone 2 reaches its maximum power density (Burnup step 5 in Table IV), the thermal flux in Zone 2 is estimated to be  $4.10 \times 10^{13}$  n/cm<sup>2</sup>-s. With this thermal flux level <sup>135</sup>Xe poisoning effects can not be ignored. Considering that the outer zone provides 41% of the total core power at the end of the cycle, the <sup>135</sup>Xe and <sup>149</sup>Sm reactivity worth is estimated to be approximately -1% and -0.2%. It is further estimated that this fission product poisoning would limit the time between fuel shuffling to approximately 0.4 year instead of 0.45 year. However, a more careful analysis is needed before firm conclusions can be drawn on the fission product effects.

The second assumption has to do with the fact that we did not account for implications associated with the production of <sup>238</sup>Pu. The <sup>238</sup>Pu is produced due to neutron capture in <sup>237</sup>Np and, to a lesser extent, in <sup>241</sup>Am; 12% of the captures in <sup>241</sup>Am result in <sup>242</sup>Cm which decays to <sup>238</sup>Pu with a 162.8-day half-life. During a 0.45 year cycle, the ATW-TZ core produces 44kg of <sup>238</sup>Pu resulting in a net production of 225% of the initial <sup>238</sup>Pu inventory. This <sup>238</sup>Pu is not mixed with the other Pu isotopes and can be recovered without a need for isotopic separation. <sup>238</sup>Pu has a commercial value as a heat source for special applications and as a radiation and thermal barrier that can make plutonium non-proliferating. Hence, its enhanced production in the ATW-TZ core might be a desirable spinoff. However, <sup>238</sup>Pu eventually decays to <sup>234</sup>U. Due to its relatively long half-life,  $2.46 \times 10^5$  years, it may have some contribution to the long term radiological hazard of the YMR. However, <sup>234</sup>U is estimated that the maximum contribution of <sup>234</sup>U to radiological hazard in the YMR is approximately 2 orders of magnitude less than that due to <sup>237</sup>Np regardless of the mobility of the medium<sup>2</sup>. Therefore, a 2.25-fold increase in <sup>238</sup>Pu inventory is not expected to reduce the beneficial effect of the dual spectrum core design approach on the long term radiological hazard of the waste coming out from the ATW.

## 6. CONCLUSIONS

The ATW-TZ core shows significant potential benefits from the dual-spectrum design. The hard spectrum inner zone maintains the desirable characteristics of the reference design while the soft spectrum outer zone efficiently burns <sup>237</sup>Np and <sup>241</sup>Am and flattens the burnup reactivity swing. This latter feature can be utilized either for extending the irradiation cycle time (thus further

enhancing the transmutation efficiency of the  $^{237}\text{Np}$  and its precursors) or for reducing the power and cost of the accelerator.

The reference design results in a net  $^{237}\text{Np}$  and precursor transmutation fraction of 28.4% during its 0.9 year fuel cycle. Under the same time constraint, the ATW-TZ core transmutes 57.2% of the  $^{237}\text{Np}$  and precursor inventory while reducing the burnup reactivity swing by a factor of 2. For the same burnup reactivity swing ( $\Delta k_{\text{eff}} = -0.06$ ), the ATW-TZ core has a fuel-cycle length of 1.45 years and transmutes 69.4% of the  $^{237}\text{Np}$  and precursor inventories.

A thorough study is needed to more accurately quantify the performance of the ATW-TZ core and to identify an optimal realistic design of such a core.

## 7. ACKNOWLEDGEMENT

This work was funded by Los Alamos National Laboratory under contract number G1772-0018.

## REFERENCES

1. Los Alamos National Lab., Presentations Prepared for the MIT Technical Review, available at [http://www-adtt.lanl.gov:80/ATW\\_papers.html](http://www-adtt.lanl.gov:80/ATW_papers.html)
2. M.D. Lowenthal, J. Ahn, P. Chambré, E. Greenspan, W.E. Kastenber, B.H. Park, N. Stone. "Impacts of Transmutation on Repository Hazards" Proc. of the Int'l Conf. on Future Nuclear Systems, Global'99, Jackson Hole, Wyoming, Aug. 29-Sep. 3, 1999.
3. J. Ahn, "Preliminary Assessment of the Effects of ATW System Application on YM Repository Performance," Proc. of the Int'l Conf. on Future Nuclear Systems, Global'99, Jackson Hole, Wyoming, Aug. 29-Sep. 3, 1999.